

Elliptic flow of thermal photons in relativistic nuclear collisions

Rupa Chatterjee,¹ Evan S. Frodermann,² Ulrich Heinz,² and Dinesh K. Srivastava¹

¹*Variable Energy Cyclotron Centre, 1/AF Bidhan Nagar, Kolkata 700 064, India*

²*Physics Department, The Ohio State University, Columbus, OH 43210, USA*

(Dated: May 24, 2019)

We predict the transverse momentum (p_T) dependence of elliptic flow of thermal photons for Au+Au collisions at the Relativistic Heavy Ion Collider. We model the system hydrodynamically, assuming formation of a thermalized quark-gluon plasma at some early time, followed by cooling through expansion, hadronization and decoupling. Photons are emitted throughout the expansion history. Contrary to hadron elliptic flow, which hydrodynamics predicts to increase monotonically with p_T , the elliptic flow of thermal photons is predicted to first rise and then fall again as p_T increases. Photon elliptic flow at high p_T is shown to reflect the quark momentum anisotropy at early times when it is small, whereas at low p_T it is controlled by the much larger pion momentum anisotropy during the late hadronic emission stage.

PACS numbers: 25.75.-q, 12.38.Mh

Experiments performed at the Relativistic Heavy-Ion Collider (RHIC) are providing evidence for the production of quark-gluon plasma (QGP) in nuclear collisions at ultra-relativistic energies. Key findings include strong anisotropic flow of all hadronic species [1, 2, 3] and a suppression of high- p_T hadrons due to parton energy loss in the dense medium [4, 5]. Signatures of direct photon emission [6, 7, 8, 9], indicative of a hot early state, have also started emerging [10]. The emphasis of the next generation of experiments will thus necessarily shift to a more precise determination of the properties of both the QGP and the subsequent hot hadronic matter. Hydrodynamic flow, and in particular anisotropic flow in non-central collisions, provides strong evidence for the existence of a hot and dense initial state with thermal pressure [3]. Elliptic flow is generated very early, via the transformation of the initial spatial eccentricity of the nuclear overlap region into momentum anisotropies through the action of azimuthally anisotropic pressure gradients. With the passage of time, the pressure gradients equalize, and the growth of elliptic flow shuts itself off [11].

Due to their strong interactions, hadrons decouple from the system late, typically when the temperature has dropped to values around 100 MeV [3, 12]. In hydrodynamic simulations, hadrons with large transverse momenta are thus emitted from those fluid elements which have the largest (radial) flow. This is supported by the hydrodynamically predicted p_T -dependence of the elliptic flow coefficient v_2 and of the Hanbury-Brown Twiss radii [12]. Photons, on the other hand, are emitted at every stage of the collision, from the pre-equilibrium stage [8], the quark-gluon fluid, and the late hadronic matter. The thermal emission of photons from the QGP and hadronic phases is obtained [13] by integrating the thermal emission rate (which is strongly biased towards higher temperatures) over the space-time history of the system. As a result, high- p_T photons arise mostly from the hot early stage, where hydrodynamic flow is weak but

the spatial eccentricity of the source is large, whereas hadrons are emitted when the temperature is low, the flow is strong and anisotropic, but the spatial eccentricity of the fireball has mostly disappeared. The elliptic flow of photons, especially at $p_T \gtrsim 1 - 2 \text{ GeV}/c$, is therefore expected to provide a glimpse of the early part of the expansion history when the fireball is in the QGP phase, complementary to the elliptic flow of hadrons.

In fact, this last argument can be made independent of the validity of hydrodynamics. For the leading photon production processes (quark-gluon Compton scattering and quark-antiquark annihilation for high energy photons in the QGP, $\pi\pi \rightarrow \rho\gamma$ for low energy photons in the hadronic phase) it is known that, for photon energies well above the rest masses of the emitting particle, the photon production cross section peaks very strongly for momenta close to that of the emitting particle [14]. So, even without local thermal equilibrium, one expects the photon elliptic flow to track the momentum anisotropy of the photon-emitting charged particles at similar momenta. For Au+Au collisions at RHIC it is known [2, 15] that the hydrodynamic behaviour of elliptic flow begins to break down for mesons (baryons) above $p_T \simeq 1.5 \text{ GeV}/c$ ($2.3 \text{ GeV}/c$): instead of continuing to rise with p_T , as predicted by hydrodynamics [3], the elliptic flow saturates. On the other hand, the systematics of hadron production with $p_T \gtrsim 2 \text{ GeV}/c$ can be well described by quark coalescence [16]. The observations then translate into a quark elliptic flow near hadronization that breaks away from hydrodynamics above $p_T \simeq 0.75 \text{ GeV}/c$ [15]. Thus, even though ideal fluid dynamics excellently describes the bulk of particle production at RHIC, viscous corrections become significant at transverse momenta above $1 \text{ GeV}/c$ for quarks and gluons and above $2 - 3 \text{ GeV}/c$ for hadrons. We expect these non-equilibrium features to be reflected by the photons, and the hydrodynamic prediction for photon elliptic flow presented here to be only an upper limit once p_T exceeds $1 \text{ GeV}/c$. Nevertheless, the

qualitative features pointed out below are generic and expected to be robust against non-equilibrium corrections.

The photon momentum spectrum can be written as

$$E dN_\gamma/d^3p = \int [(\dots) \exp(-p \cdot u(x)/T(x))] d^4x, \quad (1)$$

where the quantity inside the square brackets indicates the thermal emission rates from the QGP or hadronic matter. $p^\mu = (p_T \cosh Y, p_T \cos \phi, p_T \sin \phi, p_T \sinh Y)$ denotes the 4-momentum of the measured photon and $u^\mu = \gamma_T (\cosh \eta, v_x(x, y), v_y(x, y), \sinh \eta)$ (with $\gamma_T = (1 - v_T^2)^{-1/2}$, $v_T^2 = v_x^2 + v_y^2$) the 4-velocity of the flow field (assuming boost-invariant longitudinal expansion [17]). We use coordinates τ, x, y, η , with volume element $d^4x = \tau d\tau dx dy d\eta$, where $\tau = (t^2 - z^2)^{1/2}$ is the longitudinal proper time and $\eta = \tanh^{-1}(z/t)$ is the space-time rapidity. The photon momentum is parametrized by its rapidity Y , its transverse momentum $p_T = (p_x^2 + p_y^2)^{1/2}$, and its azimuthal emission angle ϕ . The photon energy in the local fluid rest frame, which enters the Boltzmann and several other factors in the thermal emission rate in the combination $p \cdot u/T$, is thus given by

$$\frac{p \cdot u}{T} = \frac{\gamma_T p_T}{T} [\cosh(Y - \eta) - v_T \cos(\phi - \phi_v)], \quad (2)$$

where $\phi_v = \tan^{-1}(v_y/v_x)$ is the azimuthal angle of the transverse flow vector. Eq. (2) shows that the azimuthal anisotropy (ϕ -dependence) of the photon spectrum, conventionally characterized by its Fourier coefficients v_n (where for equal nuclei only even n contribute at $Y = 0$),

$$\frac{dN(b)}{d^2p_T dY} = \frac{dN(b)}{2\pi p_T dp_T dY} [1 + 2v_2(p_T, b) \cos(2\phi) + \dots], \quad (3)$$

is controlled by an interplay between the collective flow anisotropy and the geometric deformation of the temperature field $T(x, y, \tau)$: It obviously vanishes in the absence of radial flow, $v_T = 0$, but for nonzero v_T it can arise both from an anisotropic flow field and from an azimuthally deformed temperature field. Only if the transverse flow points radially ($\phi_v = \phi_r = \tan^{-1}(y/x)$) and both the flow and temperature fields are azimuthally symmetric ($v_T(x, y) = v_T(r)$ and $T(x, y) = T(r)$ with $r^2 = x^2 + y^2$) can the ϕ -dependence in Eq. (2) be made to disappear, by rotating under the integral (1) the transverse coordinates $(x, y) = (r, \phi_r)$ such that $\phi_r = \phi$.

We employ the boost invariant hydrodynamic code AZHYDRO [18] which has been used extensively to explore hadron production at RHIC [12]. We use standard [12, 18] initial conditions for Au+Au collisions at $\sqrt{s} = 200$ A GeV, but extrapolated from the usual initial time $\tau_0 = 0.6$ fm/c to a 3 times smaller value of $\tau_0 = 0.2$ fm/c, assuming 1-dimensional boost-invariant expansion between these times. We do so in order to account for at least a fraction of the pre-equilibrium photon

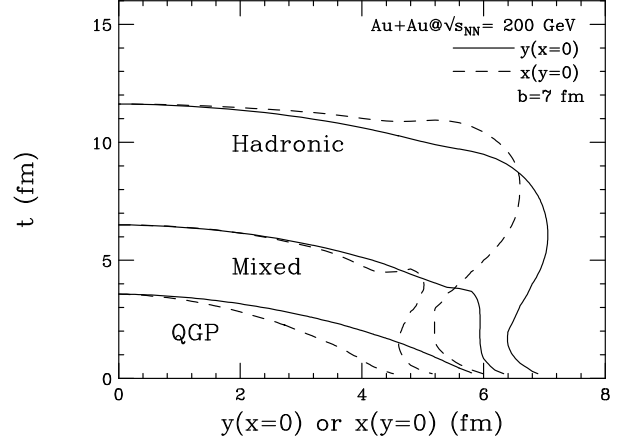


FIG. 1: Constant energy density contours for $\epsilon = \epsilon_q, \epsilon_h$, and ϵ_f , along $y(x=0)$ and $x(y=0)$, for Au+Au at $b = 7$ fm.

production at very early times [19]; its contribution to the photon spectrum is important at large p_T , and will suppress v_2^{photon} there because very little transverse flow develops before 0.6 fm/c. So our initial maximum entropy density in the center of the fireball for $b = 0$ collisions is $s_0 = 3 \times 117 \text{ fm}^{-3} = 351 \text{ fm}^{-3}$, corresponding to a peak initial temperature of $T_0 = 520$ MeV. The initial transverse entropy density profile is computed from a Glauber model assuming 75% wounded nucleon and 25% binary collision scaling of the initial entropy production [12]. This reproduces the collision centrality dependence of hadron production in Au+Au collisions at RHIC [12, 20].

We assume that a thermally and chemically equilibrated plasma is formed at the initial time and use the complete leading-order results for the production of photons from the QGP from Ref. [6] and the latest results for the radiation of photons from a hot hadronic gas obtained in Ref. [7]. These are known to provide a good description of single photon data at SPS energies and of the recent first RHIC data [9, 21, 22]. For the equation of state we use EOS Q [18] which matches a free quark-gluon gas (QGP) to a chemically equilibrated hadron resonance gas (HG) by a Maxwell construction at critical temperature $T_c = 164$ MeV, with energy densities $\epsilon_q = 1.6 \text{ GeV/fm}^3$ and $\epsilon_h = 0.45 \text{ GeV/fm}^3$ in the QGP and HG subphases at this temperature. Hadron freeze-out is assumed to happen at $\epsilon_f = 0.075 \text{ GeV/fm}^3$ [12].

Figure 1 shows the changing spatial anisotropy of the fireball, for Au+Au collisions at a typical impact parameter of $b = 7$ fm, by plotting cuts through constant energy density surfaces along the x and y -axes (i.e. in the reaction plane and perpendicular to it) for the three values ϵ_q , ϵ_h , and ϵ_f . One sees that after about 9 fm/c the initial out-of-plane deformation changes sign (dashed and solid lines cross), as a result of faster expansion into the reaction plane. Figure 2 illustrates the resulting anisotropy of the transverse flow field, by plotting the flow velocities along the same cuts. Through most of the fireball interior the velocity along the x -axis is larger and rises more

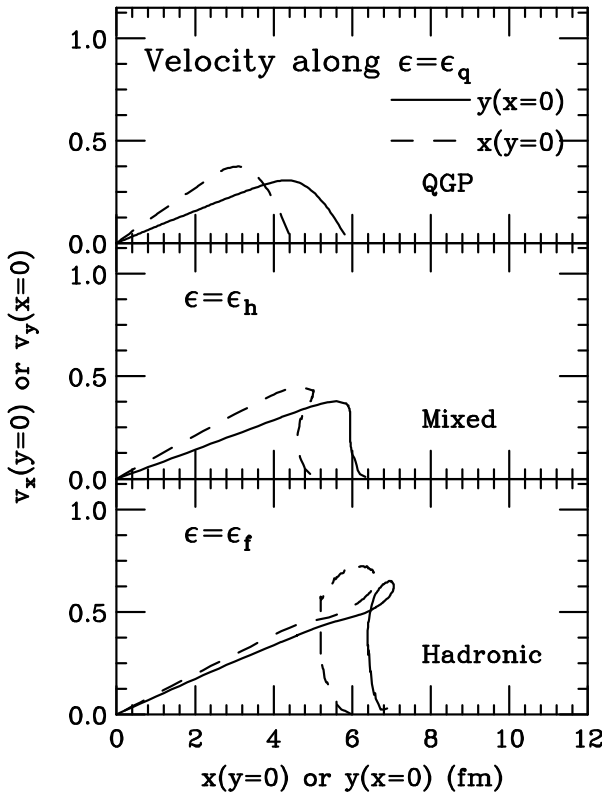


FIG. 2: Flow velocity along the constant energy density contours for $\epsilon = \epsilon_q$ (QGP phase, upper panel), ϵ_h (mixed phase, middle panel), and ϵ_f (hadronic phase, lower panel) for $y(x=0)$ and $x(y=0)$, for 200 A GeV Au+Au at $b = 7$ fm.

rapidly with increasing radius than along the y -axis. At hadronic freeze-out, ϵ_f , the in-plane and out-of-plane velocity gradients have almost (but not fully!) equalized and larger in-plane flow velocities exist mostly near the fireball surface. Figure 2 complements similar plots in Refs. [3, 12] which show velocity profiles either at constant time or only along the freeze-out surface at $b = 0$.

Our results for thermal photon elliptic flow for $b = 7$ fm are shown in Fig. 3. We compare the overall $v_2(p_T)$ with the individual elliptic flow parameters associated with the quark matter ($v_2(QM)$) and hadronic matter ($v_2(HM)$) contributions to the thermal photon spectrum. Comparison of the latter with the elliptic flow of thermal pions ($v_2(\pi)$, see Fig. 3) shows how hadronic photon momenta track pion momenta. The somewhat lower photon elliptic flow ($v_2(HM) < v_2(\pi)$) can be attributed to the earlier emission of the average hadronic photon compared to the pions whose momentum anisotropy continues to slightly increase during the hadronic stage. We have no good explanation for the structure in the v_2 of hadronic photons around $p_T \sim 0.25$ GeV/ c , which generates a similar peak in the overall photon elliptic flow, except that it seems to arise from a strong energy dependence of the hadronic photon emission rates in the low- p_T region.

The elliptic flow of the QGP photons, $v_2(QM)$, is small

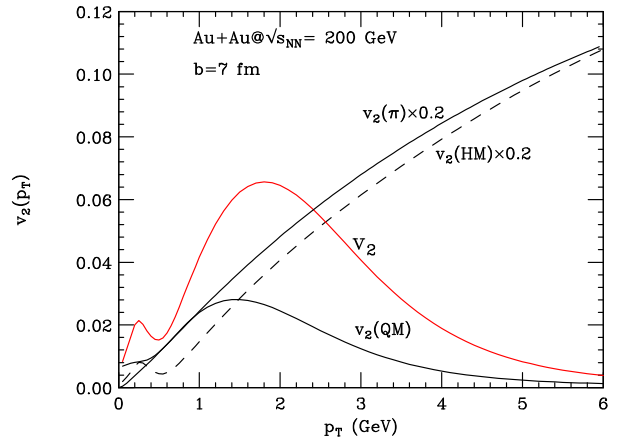


FIG. 3: $v_2(p_T)$ for thermal photons from 200 A GeV Au+Au collisions with $b = 7$ fm impact parameter. Quark and hadronic matter contributions are also shown separately, and the elliptic flow of pions is shown for comparison.

at low p_T , peaks around $p_T \sim 1.5$ GeV/ c , and decreases again for large p_T . Its smallness at high p_T and increase towards lower p_T reflects the absence of transverse flow during the earliest, hottest stage of the QGP and its gradual buildup during the following cooler stages. That growth is cut off by the generic decrease of v_2 as $p_T \rightarrow 0$ [23]. Its nonzero limit at $p_T = 0$ (first observed in [24] for gluons) can be traced to the singularities of the Bose distribution and emission rates at $p_T = 0$. Since the QGP photon rates [6] are unreliable for $p_T < 0.2$ GeV/ c , the dashed curve in Fig. 3 should not be trusted in that domain. Fortunately, there the total v_2 (solid line) is entirely dominated by the hadronic photon contribution.

Although the hydrodynamically predicted elliptic flow of hadronic photons is almost everywhere much larger than that of the QGP photons, the hadronic contribution to the photon spectrum is increasingly suppressed (by more than an order of magnitude) below the QGP contribution once p_T exceeds 1.5–2 GeV/ c . Hence the overall photonic v_2 , while larger than the pure QGP contribution, also decreases for large p_T , approaching the v_2 of the QGP photons. At high p_T the photon elliptic flow thus opens a window onto the dynamics of the QGP, in spite of the larger elliptic flow of the hadronic photons.

In Figure 4 we present the impact parameter dependence of the elliptic flow of thermal photons. The impact parameters are chosen to roughly correspond to collision centralities of 0–10%, 10–20%, 20–30%, 30–40%, 40–50%, and 50–60% of the total inelastic nuclear cross section. As the impact parameter increases, the relative contribution of hadronic photons increases, too. Since its elliptic flow is larger than that of the QGP photons, the impact parameter dependence of thermal photon v_2 is predicted to be stronger than that of hadron v_2 . This can be used as an additional tool to isolate the QGP contribution to thermal photon emission, espe-

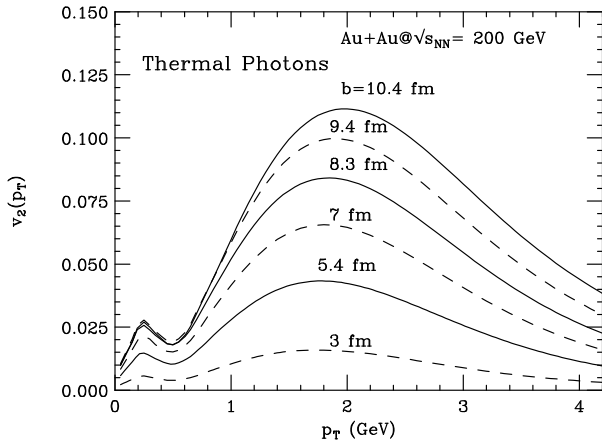


FIG. 4: Impact parameter dependence of the azimuthal anisotropy of thermal photons.

cially if methods can be developed [25] to subtract the hadronic contribution $v_2(\text{HM})$ from the thermal photon elliptic flow, by exploiting its similarity to the elliptic flow of thermal pions.

However, a quantitative interpretation of photon elliptic flow in the context of extracting dynamical information on the QGP evolution must also account for other contributions to high- p_T photon production. It has recently been argued that jets passing through the QGP contribute significantly to direct photon production at large p_T [9] and may even lead to negative photon elliptic flow in this region [26]. These calculations neglect, however, the anisotropic collective flow of the plasma. It would be interesting to see how much of the effects predicted in [26] survives once they are properly combined with the collective flow study presented here.

In conclusion, we have presented a first calculation of elliptic flow of thermal photons, emitted from ultrarelativistic collision of heavy nuclei. The azimuthal flow parameter exhibits a rich structure as a function of transverse momentum, driven by the evolution of the system and the competing rates of photon emission from the quark and hadronic matter stages. Its impact parameter dependence differs from that of pion elliptic flow since the relative contributions of hadronic and quark matter emissions change with collision centrality. Finally, we have argued that the elliptic flow of thermal photons from the hadronic matter tracks the flow of pions, which can be estimated independently and possibly subtracted. This may open a previously unanticipated window into the study of the buildup of collective flow in the QGP. Similar considerations should apply to thermal dilepton emission. Without doubt such a study would be very valuable.

This work was supported by the U.S. Department of Energy under contract no. DE-FG02-01ER41190.

[1] C. Adler *et al.* [STAR Collaboration], Phys. Rev. Lett. **87** 182301 (2001); *ibid.* **89** 132301 (2002); J. Adams *et al.* [STAR Collaboration], *ibid.* **92**, 052302 (2004); K. Adcox *et al.* [PHENIX Collaboration], *ibid.* **89**, 212301 (2002).

[2] C. Adler *et al.* [STAR Collaboration], Phys. Rev. Lett. **90**, 032301 (2003); S. S. Adler *et al.* [PHENIX Collaboration], *ibid.* **91**, 182301 (2003).

[3] P. F. Kolb, J. Sollfrank and U. Heinz, Phys. Rev. C **62**, 054909 (2000); P. Huovinen, P. F. Kolb, U. Heinz, P. V. Ruuskanen and S. A. Voloshin, Phys. Lett. B **503**, 58 (2001); D. Teaney, J. Lauret and E. V. Shuryak, nucl-th/0110037.

[4] X. N. Wang, Phys. Rev. C **63**, 054902 (2001); M. Gyulassy, I. Vitev, X. N. Wang, Phys. Rev. Lett. **86**, 2537 (2001).

[5] K. Adcox *et al.* [PHENIX Collaboration], Phys. Rev. Lett. **88**, 022301 (2002); J. Adams *et al.* [STAR Collaboration], *ibid.* **91**, 172302 (2003).

[6] P. Arnold, G. D. Moore, and L. G. Yaffe, JHEP **0112**, 009 (2001).

[7] S. Turbide, R. Rapp, and C. Gale, Phys. Rev. C **69**, 014903 (2004).

[8] S. A. Bass, B. Müller, and D. K. Srivastava, Phys. Rev. Lett. **90**, 082301 (2003); Phys. Rev. C **66**, 061902 (2002); T. Renk, S. A. Bass, and D. K. Srivastava, Phys. Lett. B (in press).

[9] R. J. Fries, B. Müller and D. K. Srivastava, Phys. Rev. Lett. **90**, 132301 (2003); R. J. Fries, B. Müller, and D. K. Srivastava, Phys. Rev. C **72**, 041902 (R) (2005).

[10] S. S. Adler *et. al.* [PHENIX Collaboration], Phys. Rev. Lett. **94**, 232301 (2005).

[11] H. Sorge, Phys. Rev. Lett. **78**, 2309 (1997); *ibid.* **82**, 2048 (1999).

[12] P. F. Kolb and U. Heinz, in *Quark-Gluon Plasma 3*, edited by R.C. Hwa and X.-N. Wang (World Scientific, Singapore, 2004), p. 634 [nucl-th/0305084].

[13] J. Alam, D. K. Srivastava, B. Sinha, and D. N. Basu, Phys. Rev. D **48**, 1117 (1993).

[14] C. Y. Wong, *Introduction to High-Energy Heavy-Ion Collisions* (World Scientific, Singapore, 1994), pp. 382–424.

[15] U. Heinz, AIP Conf. Proc. **739**, 163 (2005).

[16] V. Greco, C. M. Ko and P. Levai, Phys. Rev. Lett. **90**, 202302 (2003); R. J. Fries, B. Müller, C. Nonaka and S. A. Bass, *ibid.* **90**, 202303 (2003); D. Molnar and S. A. Voloshin, *ibid.* **91**, 092301 (2003).

[17] J. D. Bjorken, Phys. Rev. D **27**, 140 (1983).

[18] The code can be downloaded from URL <http://nt3.phys.columbia.edu/people/molnare/OSCAR/>. See also the first paper in [3], and P. F. Kolb and R. Rapp, Phys. Rev. C **67**, 044903 (2003).

[19] S. A. Bass, B. Müller and D. K. Srivastava, Phys. Rev. Lett. **93**, 162301 (2004).

[20] A. J. Kuhlman and U. Heinz, Phys. Rev. C **72**, 037901 (2005).

[21] D. K. Srivastava, Phys. Rev. C **71**, 034905 (2005).

[22] D. d'Enterria and D. Peressounko, nucl-th/0503054.

[23] P. Danielewicz, Phys. Rev. C **51**, 716 (1995).

[24] U. Heinz and S. Wong, Phys. Rev. C **66**, 014907 (2002).

[25] S. Adler *et al.* [PHENIX Collaboration], nucl-ex/0508019.

[26] S. Turbide, C. Gale, and R. J. Fries, hep-ph/0508201.